The Journal of Neuroscience, January 15, 1996, 16(2):519–530

Developmental Regulation of the Toxin Sensitivity of Ca^{2+}-Permeable AMPA Receptors in Cortical Glia

Olimpia Meucci, Alessandro Fatatis, James A. Holzwarth, and Richard J. Miller

Department of Pharmacological and Physiological Sciences, The University of Chicago, Chicago, Illinois 60637

We examined the properties of glutamate agonist-induced Ca^{2+} fluxes in cultured CG-4 and O-2A progenitor cells from rat cortex. Kainate-induced Ca^{2+} fluxes in these cells were found to be attributable to the activation of AMPA receptors. Thus, these fluxes were enhanced by cyclothiazide but not by concanavalin A and were blocked completely by GYKI-53655. We simultaneously examined kainate-induced Ca^{2+} entry and Na^{+} currents in these cells under voltage-clamp conditions. Both of these parameters were blocked by Joro spider toxin (JSTx) in undifferentiated cells. However, neither JSTx nor Argiotoxin 636 effectively blocked either parameter in cells differentiated into type II astrocytes. This change in toxin sensitivity occurred slowly over a period of several days. Similar results were obtained in Ca^{2+}-imaging studies. When cells were differentiated into oligodendrocytes, they showed an intermediate sensitivity to block by JSTx as assessed using imaging and voltage-clamp studies. Analysis of the expression of AMPA-receptor subunits showed an increase in the concentration of glutamate receptor-2 (GluR2) in CG-4 cells as they differentiated into type II astrocytes and oligodendrocytes. These results demonstrate that the AMPA receptors in cells of the O-2A lineage flux appreciable amounts of Ca^{2+} but may contain variable amounts of edited GluR2 subunits.

Key words: glia; glutamate receptors; ion channels; Ca permeability; development; Jorotoxin; CG-4 cells

Glutamatergic excitatory synaptic transmission in the brain is mediated by many different types of glutamate receptors (Hollmann and Heinemann, 1994; McBain and Mayer, 1994; Miller, 1994). Indeed, the ultimate diversity of these receptors is still unknown. One particularly important property of ionophore-linked glutamate receptors is their permeability to Ca^{2+}. Thus, Ca^{2+} is known to be of great importance in mediating many of the effects of glutamate on neuronal excitability, plasticity, and viability (Choi and Rothman, 1990; Bliss and Collingridge, 1993). Initially, it was thought that only NMDA receptors exhibited high Ca^{2+} permeability, whereas "non-NMDA" receptors essentially were Ca^{2+}-impermeable (MacDermott et al., 1986; Mayer et al., 1987); however, the situation was significantly more complex. Both biophysical and molecular biological studies demonstrated that some non-NMDA receptors also appeared to flux Ca^{2+} very well (Murphy and Miller, 1989a,b; Iino et al., 1990; Gilbertson et al., 1991; Brorson et al., 1992; Lerma et al., 1994; Geiger et al., 1995). One important determinant of the Ca^{2+} permeability of AMPA receptors appears to be the presence of an edited version of the GluR2 subunit [GluR2(R)]. Experiments examining the properties of recombinant AMPA receptors have shown that the absence of GluR2(R) allows the formation of receptors for which Ca^{2+} permeability is high and can approach that of NMDA receptors (Hollmann et al., 1991; Hume et al., 1991; Burnashev et al., 1992a,b, 1995).

The question remains, however, as to the subunit structure of naturally occurring AMPA receptors that differ in their abilities to flux Ca^{2+}. In one striking example, that of the Bergmann glial cells of the cerebellum, it is clear that the AMPA receptors lack GluR2(R) and exhibit the predicted high Ca^{2+} permeability (Burnashev et al., 1992a; Müller et al., 1992; Geiger et al., 1995). Such a complete lack of GluR2(R) in cells may be relatively rare (Lambolez et al., 1992; Jonas et al., 1994, Geiger et al., 1995); however, many types of cells now are known to exhibit AMPA receptors with relatively high Ca^{2+} permeabilities (Schneggenburger et al., 1993a,b; Zeilhofer et al., 1993; Jonas et al., 1994) (see Discussion). One such example occurs in cells of the O-2A progenitor lineage that can differentiate *in vitro* into oligodendrocytes or type II astrocytes (Louis et al., 1992; Holzwarth et al., 1994). These cells also possess pronounced kainate-activated Ca^{2+} and Co^{2+} fluxes, although it is clear that they also express GluR2(R) (Holzwarth et al., 1994; Patneau et al., 1994; Puchalski et al., 1994). We hypothesized that the cells contain a "mosaic" of AMPA receptors, some of which are formed without GluR2(R). We speculated that these receptors are responsible for a majority of the Ca^{2+} flux observed, the Na^{+} current being dominated by GluR2(R)-containing "Ca^{2+}-impermeable" receptors. The existence of such AMPA-receptor mosaics has been detected in other studies (Burnashev et al., 1992b; Geiger et al., 1995). It was demonstrated previously that certain spider toxins, including Joro spider toxin (JSTx) and Argiotoxin 636, selectively block AMPA receptors that lack GluR2(R) and, therefore, exhibit a high Ca^{2+} permeability (Blaschke et al., 1993; Herlitze et al., 1993). We have examined in this study the effects of these toxins on Ca^{2+}-permeable AMPA receptors in cells of the O-2A lineage. Surprisingly, although cells at various stages of development possess AMPA receptors that are appreciably Ca^{2+}-permeable, their sen-

Received June 7, 1995; revised Oct. 10, 1995; accepted Oct. 17, 1995.

This research was supported by Public Health Service Grants DA-02121, DA-02575, MH-40165, and NS-21442. O.M. was supported by l'Associazione per la Promozione delle Ricerche Neurologiche (Arin, 1993) and by Ministero della Sanitá, Italy (borsa AIDS, 1994). We thank Dr. Vittorio Gallo for providing CG-4 cell line and for other helpful advice.

Correspondence should be addressed to Richard J. Miller, Department of Pharmacological and Physiological Sciences, The University of Chicago, 947 East 58th Street, Chicago, IL 60637.

Dr. Holzwarth's present address: Strasbourg Research Center, 16 Rue d'Ankara, 67080 Strasbourg Cedex, France.

sitivity to spider toxins changes dramatically, suggesting a switch in their subunit structure.

MATERIALS AND METHODS

Kainic acid and cyclothiazide were purchased from Sigma (St. Louis, MO). Fura-2 AM and pentapotassium salt were purchased from Molecular Probes (Eugene, OR). JSTx was purchased from Research Biochemicals (Natick, MA). Argiotoxin was purchased from Accurate Chemical and Scientific (Westbury, NY). Thapsigargin was purchased from LC Laboratories (Woburn, MA). Anti-A2B5 and anti-galactocerebroside (anti-GalC) monoclonal antibodies were purchased from Boehringer Mannheim (Mannheim, Germany). Anti-glial fibrillary acidic protein (anti-GFAP) polyclonal antibody was purchased from Accurate Chemical and Scientific. The secondary antibodies conjugated with Texas red and fluorescein isothiocyanate (FITC) fluorochrome were purchased from Jackson Immunoresearch (West Grove, PA). GYKI-53655 was a generous gift of Eli Lilly (Indianapolis, IN). All other chemicals were purchased from local suppliers and were of reagent grade.

Cell cultures. O-2A progenitor-enriched primary cultures were obtained as described previously (McCarthy and de Vellis, 1980), with modifications. Briefly, 1- to 2-d-old Holtzman rat pups were decapitated, and the brains were removed and transferred in fresh HBSS (Life Technologies, Gaithersburg, MD). The meninges and hippocampus were removed and discarded. The tissue was chopped into 1 mm pieces. After two washes with HBSS, the tissue was incubated with 0.25% trypsin (20–25 min at 37°C). After incubation, the tissue was washed twice with fresh HBSS to remove trypsin, and DMEM + 10% fetal calf serum (FCS) was added. Then the cells were triturated gently in the presence of DNase (200 μl/2 ml HBSS from a stock solution prepared as follows: 3 mg of DNase + 5 mg of $MgSO_4$ in 2 ml of HBSS) with a sterile Pasteur pipette. Dispersed cells were collected in a tube containing DMEM + 10% FCS, and the remaining tissue was triturated until no clumps were visible and then moved to the same tube. Cells were plated in 75 cm^2 culture flasks in DMEM + 10% FCS + gentamycin (50 mg/l) and allowed to grow until confluent. At ~10 d in culture, macrophages were detached and discarded by a 6 hr shaking at 200 rpm, and O-2A progenitors cells growing on the top of a confluent monolayer of astrocytes were detached by an additional shaking for 18 hr at 200 rpm. Cells were grown as O-2A progenitors in a chemically defined, serum-free medium containing 30% B-104-conditioned medium and 10 ng/ml biotin and N1 supplement (Louis et al., 1992) for 2–5 d before the experiments. For differentiation into type II astrocytes or oligodendrocytes, cells were grown for 7–10 d in 10% FCS DMEM or 2% FCS DMEM + N1 supplement and biotin, respectively.

CG-4 cells were grown as progenitors in the same chemically defined, serum-free medium used for primary cultures of O-2A progenitors. Differentiation into type II astrocytes was achieved by culturing the cells in 20% FCS DMEM containing 10 ng/ml biotin for 7–10 d and then maintaining the cells in 10% FCS DMEM (Louis et al., 1992). Mature oligodendrocytes ($GalC^+$) were obtained by culturing the cells in 2% FCS DMEM + N1 supplement and biotin for 7–10 d.

All cells were plated on 100 mm plastic petri dishes coated with poly-D-ornithine (100 μg/ml). Cells were plated onto 25 mm round glass coverslips coated with poly-D-ornithine 2 or 3 d before the experiments. Differentiation of oligodendrocytes was started directly on glass coverslips.

Immunofluorescence. Primary cultures enriched in O-2A progenitors or type II astrocytes/oligodendrocytes were characterized immunocytochemically. After fixation with 4% *p*-formaldehyde (30 min at room temperature), cells were incubated with monoclonal anti-A2B5 antibody for 30 min and then incubated with goat anti-mouse Texas red-conjugated antibody (30 min). For GFAP, cells were permeabilized with 0.2% Tween-20 for 45 min and then incubated with the rabbit polyclonal anti-GFAP antibody for 30 min, followed by a 30 min incubation with donkey anti-rabbit FITC-conjugated antibody. For GalC, cells were fixed as described above, incubated with monoclonal anti-GalC antibody for 30 min, and then incubated with goat anti-mouse Texas red-conjugated antibody for 30 min.

All cultures were examined using a Leitz Diaplan microscope equipped with fluorescence optics. Primary cultures enriched in O-2A progenitor cells were 95% positive for A2B5, whereas 75% of the cells in type II astrocyte cultures stained positively for both A2B5 and GFAP. The percentage of $GalC^+$ cells in cortical glia cultured in 2% FCS was 60%.

Fura-2 video imaging. The cells were loaded with 2 μM Fura-2 acetoxymethylester using a balanced salt solution (standard buffer) of the

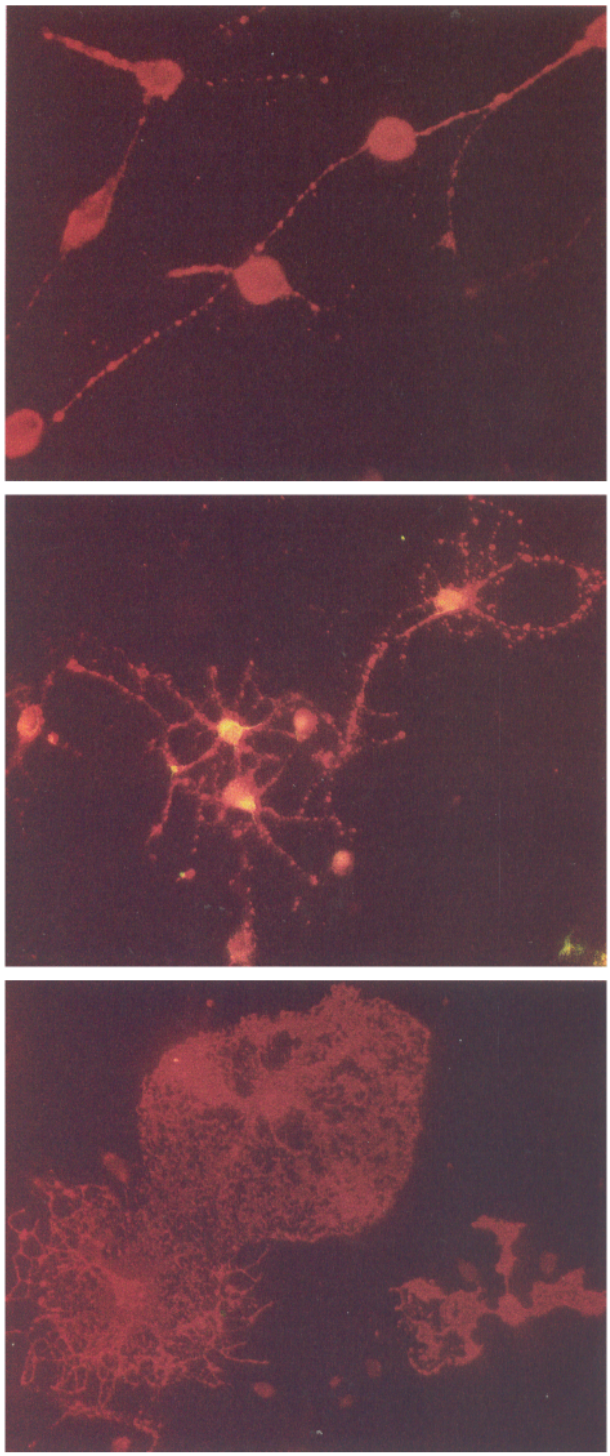

Figure 1. Immunofluorescence staining for A2B5 (Texas red), GFAP (FITC), and GalC (Texas red) was performed on primary cortical glial cultures to identify (*top*) O-2A progenitors ($A2B5^+/GFAP^-$), (*middle*) type II astrocytes ($A2B5^+/GFAP^+$), and (*bottom*) oligodendrocytes ($GalC^+$). Cells were grown in a defined serum-free medium or in the presence of FCS, as described in Materials and Methods. As expected, almost all of the cells (>95%) cultured in the serum-free medium stained only with anti-A2B5 antibody and showed the morphological features of glial progenitors, whereas >75% of the cells grown in the presence of 20% serum for 2 weeks stained positively with both anti-A2B5 and anti-GFAP antibodies ($n = 96$) and morphologically resembled type II astrocytes. Cells cultured in 2% FCS N1-defined medium for 5–10 d were positive for GalC (60%, $n = 127$). Magnification, 300× (*top*) and 250× (*middle* and *bottom*).

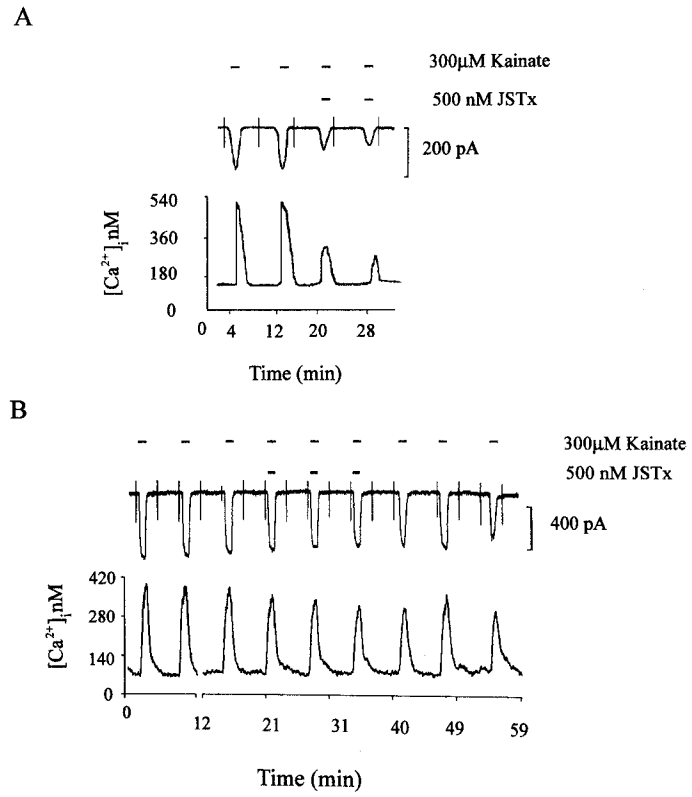

Figure 2. Effect of JSTx on the kainate-activated current and $[Ca^{2+}]_i$ increase recorded simultaneously under voltage-clamp conditions (holding potential −80 mV) from an O-2A progenitor cell (*A*) and a type II astrocyte (*B*).

following composition (in mM): 159 NaCl, 5 KCl, 0.4 $MgSO_4$, 0.5 $MgCl_2$, 0.64 KH_2PO_4, 3 $NaHCO_3$, 20 HEPES, 5 glucose, 0.33 Na_2HPO_4, 2 $CaCl_2$, and bovine serum albumin (BSA) 0.2% (330 mOsm/kg), pH-adjusted to 7.35 with 1 M Tris. The cells were incubated with Fura-2 for 30 min at room temperature to avoid probe compartmentalization and then incubated for an additional 15 min at room temperature to allow de-esterification of the Fura-2 dye.

Coverslips were mounted on a coverslip chamber (Medical Systems, Greenvale, NY) for fluorescence measurements. Gridded square coverslips (Bellco Glass, Vineland, NJ) were used when indicated, and immunocytochemistry was performed on the same cells of the Ca^{2+} experiment to correlate directly the Ca^{2+} response to the developmental stage. All measurements were made at room temperature, and the experiments were performed in a Na^+-free standard buffer containing *N*-methyl-D-glucamine (NMDG; 157 mM) to abolish Na^+-dependent depolarization. In some experiments, an increase in intracellular Ca^{2+} concentration ($[Ca^{2+}]_i$) was obtained with Na^+-free solutions per se; unless the $[Ca^{2+}]_i$ returned to baseline, these experiments were not included in data analysis. For the Ca^{2+}-free experiments, Ca^{2+} was omitted and 0.2 mM EGTA was added. Both Na^+- and Ca^{2+}-free solutions were perfused for 4 min before starting the experiments. Cells were superfused continuously using a peristaltic pump (Gilson, Villiers Le Bel, France; flow rate 650 μl/min), and the perfusion medium was perfused directly onto the cells under observation by a microtube that was positioned with a macromanipulator (Narishige, Greenvale, NY). Removal of experimental solutions from the coverslip chamber (500 μl vol) was achieved using a microaspirator (Medical Systems) connected to a vacuum pump. A two-way valve (Thomson, Springfield, VA) controlled the flow from a separate injection-loop that was used to perfuse cells with different experimental solutions.

The cytoplasmic fluorescence appeared to be uniform throughout the cells. Fura-2 fluorescence was imaged with an inverted Nikon Diaphot microscope using a Nikon 20× Fluor objective lens. The cells were illuminated with a 150 W Xenon lamp (Osram, Rochester, NY) with quartz collector lenses. A shutter and a filter wheel containing the two different interference filters (340 and 380 nm) were controlled by a computer. Emitted light passed through a 480 nm barrier filter into a KS1380 image intensifier coupled to a Dage model 70 Vidicon camera (MTI, Michigan City, IN). Images were averaged (16 frames/data point) and then digitized in an image processor (Applied Imaging, Dukesway Gateshead, UK) connected to a 486 PC equipped with TARDIS software. Each cell in the image was analyzed independently for each time point in the captured sequence. All individual cell $[Ca^{2+}]_i$ traces shown are representative responses for a given field of cells. For the calibration of fluorescent signals, we used cells loaded with Fura-2. Ratios at saturating and zero Ca^{2+} (R_{max} and R_{min}, respectively) were obtained by perfusing cells with standard buffer containing 10 mM $CaCl_2$ and 4 μM ionomycin and subsequently with a Ca^{2+}-free solution containing 10 mM EGTA. The obtained R_{max} and R_{min} values, expressed as gray-level mean, were used to calculate the calibration curve using TARDIS software. The $[Ca^{2+}]_i$ was determined according to the equation of Grynkiewicz et al. (1985).

Simultaneous Fura-2 microfluorimetry and electrophysiology. Cells were plated on coverslips 3 d before the experiment, and Fura-2 was supplied by the patch pipette. Coverslips were mounted in a laminar flow perfusion chamber (flow rate 2–2.5 ml/min). The light from a 150 W Xe arc lamp was passed through a dual-beam spectrophotometer (Phoenix Instruments, Phoenix, AZ), which alternated wavelengths from 340 to 380 nm using a chopper spinning at 60 Hz. The emission fluorescence was passed through a 480 nm barrier filter, and the recording area was isolated with a rectangular diaphragm. The average intensity values for each wavelength were stored. After the completion of an experiment, a background was taken in an area with no cells or debris. Ratios were converted to free $[Ca^{2+}]_i$ by using the equation $[Ca^{2+}] = K(R - R_{min})/(R_{max} - R)$, where R is the 340/380 nm fluorescence ratio according to Grynkiewicz et al. (1985). R_{max}, R_{min}, and the constant K were determined from a standard curve generated using Fura-2-free acid in solutions of known $[Ca^{2+}]_i$. Whole-cell patch-clamp measurements were performed as described previously (Thayer et al., 1988). Currents were amplified by an EPC7 patch-clamp amplifier (List Biologicals, Campbell, CA) and recorded by a chart recorder attached to the output from an 8-pole Bessel filter. Cells were held at −80 mV. A sweep from −80 to 0 mV of 520 msec duration was performed every 3 or 4 min (which is seen as a vertical spike on the current record). Na^+-containing solutions were as described above. The intracellular solutions contained the following: 100 mM CsCl, 40 mM CsF, 1 mM $MgCl_2$, 10 mM HEPES, 3.6 mM Mg-ATP, 14 mM Tris, 2 mM creatine phosphate, 50 U/ml creatine phosphokinase, 200 μM Fura-2, 320 mOsm, pH 7.3. Cells were accepted for study if a stable seal formed and the cell input resistance was at least 150 MΩ formed. Patch pipettes of 2.5–4.5 MΩ were used. Agonists were applied by bath application. All experiments were performed at room temperature.

Western blot analysis. Total proteins were obtained from CG-4 cells using a lysis buffer of the following composition: 50 mM Tris-HCl, 1 mM EDTA, 1 mM EGTA, 200 μM phenylmethylsulfonylfluoride, and 40 μM leupeptin. Samples from undifferentiated (O-2A progenitors) and differentiated (type II astrocytes and oligodendrocytes) cells were run on minigels [SDS-PAGE 7.5% acrylamide, 5.5 (length) × 8.5 (width) cm], as described by Laemmli et al. (1970). The total amount of proteins was determined by using the Micro BSA protein assay Reagent Kit (Pierce, Rockford, IL), and 30 μg of proteins was run in each lane. Proteins were transferred to nitrocellulose membrane (Towbin et al., 1979), and detection of glutamate receptor subunits was performed after blocking the membrane for 1 hr at room temperature in blocking buffer (5% low-fat milk/2% BSA/0.1 Tween in PBS). Immunoblots were incubated with affinity-purified monoclonal (anti-GluR2) or polyclonal (anti-GluR3, anti-GluR4) antibodies for 1 hr at room temperature in blocking buffer. Primary antibodies were diluted in blocking buffer and used at 1:10 (for GluR2), 1:1000 (for GluR3), and 1 μg/ml (for GluR4) dilution. Anti-GluR2 and -GluR3 were a generous gift of Dr. Scott Rogers (The University of Utah), and anti-GluR4 was purchased from Upstate Biotechnology (Lake Placid, NY). After washing in 0.1% Tween/PBS (two changes of buffer, one 15 min wash, and two 5 min washes), immunoblots were incubated with horseradish peroxidase-conjugated goat anti-mouse or anti-rabbit IgG (1:20,000; Promega, Madison, WI) for 1 hr at room temperature. After washing as indicated above, the detection of protein was visualized with enhanced chemiluminescence (Amersham, Buckinghamshire, UK). The densitometric analysis was performed by using a scanner connected to a BioImage system (Millipore, Bedford, MA).

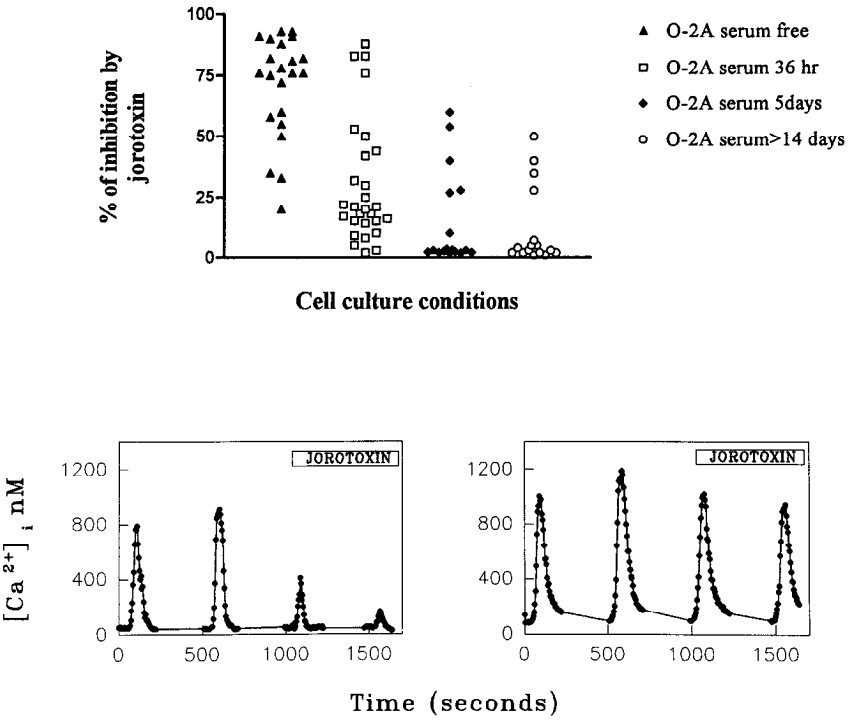

Figure 3. *Top*, Changes in the sensitivity of peak kainate (300 μM)-induced $[Ca^{2+}]_i$ responses to JSTx (500 nM) block on differentiation of O-2A progenitor cells into type II astrocytes (Na^+-free conditions). Each data point is from a single cell. The inhibition of kainate response induced by JSTx was 70 ± 5% in O-2A progenitors (▲; $n = 22$), 30 ± 4% 36 hr after the addition of serum (□; $n = 28$, $p < 0.05$ vs O-2A progenitors), 17 ± 5% after 5 d of serum (◆; $n = 18$, $p < 0.05$ vs O-2A progenitors), and 12 ± 4% after 2 weeks of serum (○; $n = 18$, $p < 0.05$ vs O-2A progenitors). Traces (*bottom*) are representative of the two different responses obtained in O-2A progenitors (*left*) and type II astrocytes (*right*) (Na^+-free conditions).

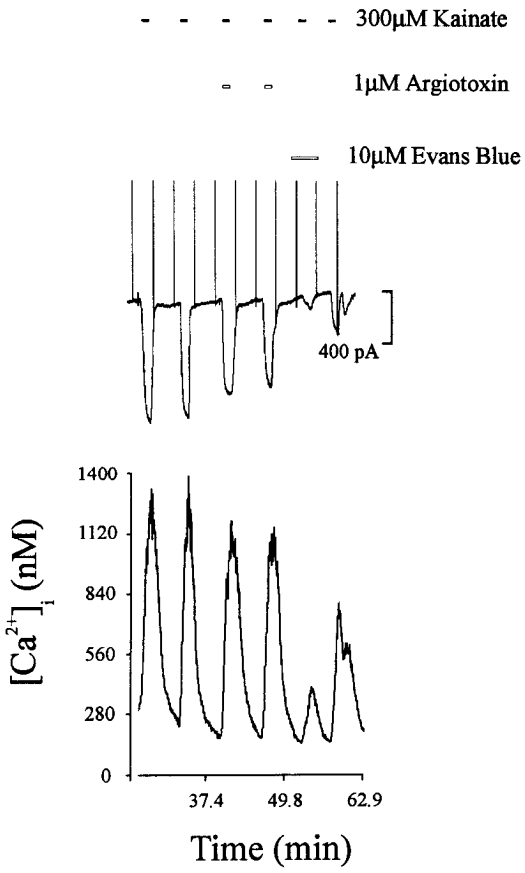

Figure 4. Example illustrates the effects of Argiotoxin 636 and Evans blue on the kainate-activated membrane current and $[Ca^{2+}]_i$ increase recorded simultaneously under voltage clamp in a type II astrocyte (holding potential −80 mV).

RESULTS

General properties of kainate-activated Ca^{2+} fluxes in cultured O-2A progenitor cells

We used two techniques for examining Ca^{2+} fluxes in cultured O-2A progenitors, type II astrocytes and oligodendrocytes from rat cortex (Fig. 1). The first of these was Fura-2 video imaging of cells, and the second was to examine kainate-induced Na^+ currents and Ca^{2+} fluxes simultaneously under voltage-clamp conditions (Thayer et al., 1988). In voltage-clamp experiments using either O-2A progenitors or type II astrocytes or oligodendrocytes, the addition of kainate elicited inward currents in normal Na^+-containing solutions that were accompanied by substantial $[Ca^{2+}]_i$ signals (Fig. 2) (see below for oligodendrocytes). These voltage-clamp studies suggest that the Ca^{2+} influx observed was attributable to the direct movement of Ca^{2+} through the kainate-gated ionophore itself and not to influx through voltage-dependent Ca^{2+} channels activated by kainate-induced depolarization. The

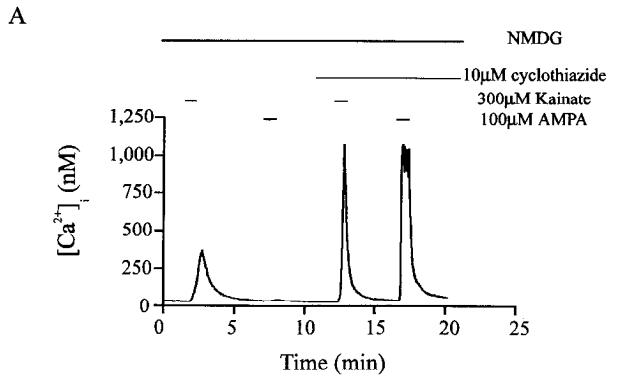

Figure 5. Effect of cyclothiazide on AMPA and kainate-induced $[Ca^{2+}]_i$ increases in a type II astrocyte determined using Fura-2 video imaging (Na^+-free conditions). Cyclothiazide caused a very large enhancement of both AMPA and kainate effects.

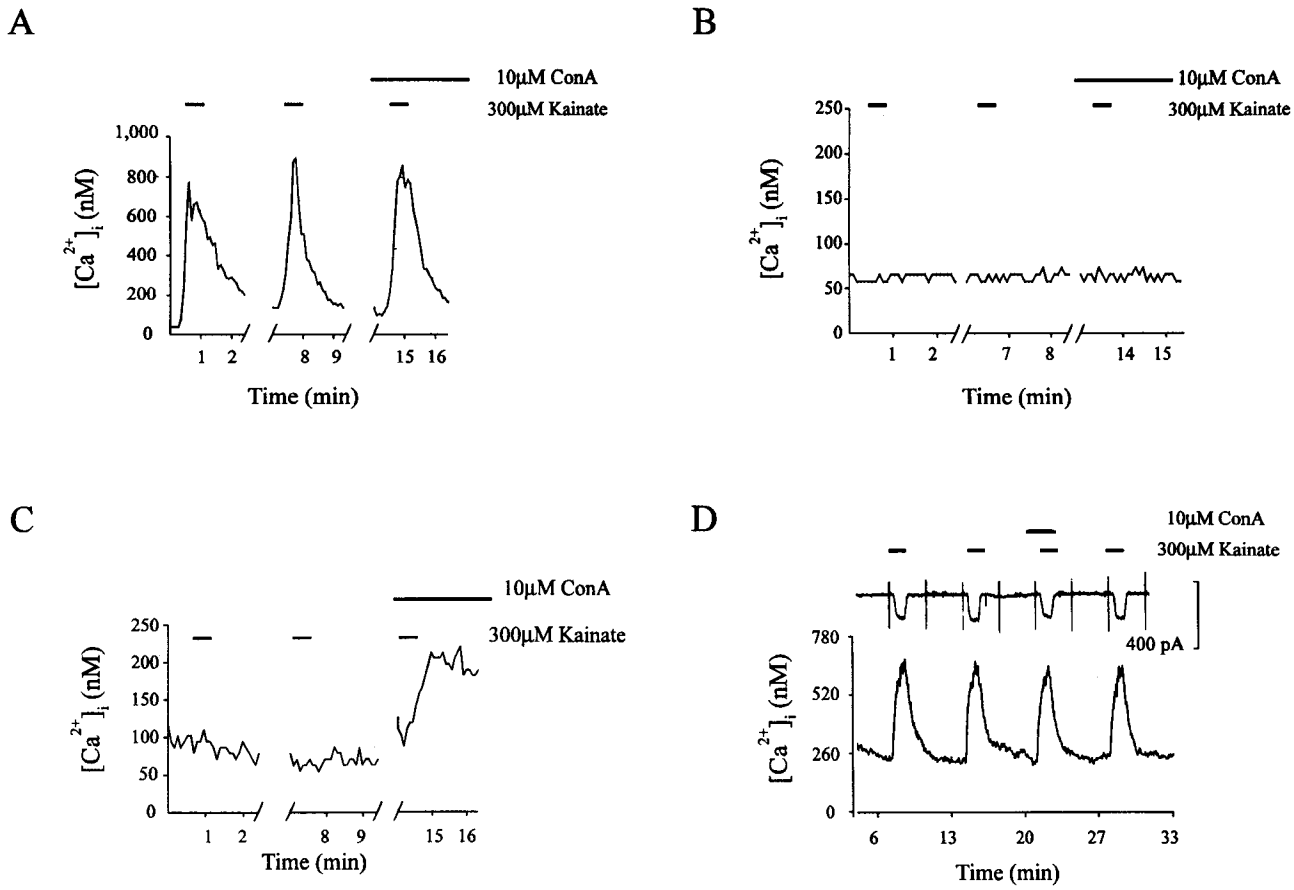

Figure 6. Effect of Con A on responses of type II astrocytes to kainate. *A–C*, When examined in a large number of cells using Fura-2 video imaging, the $[Ca^{2+}]_i$ response to kainate usually was not altered by Con A (Na^+-free conditions). This is shown in *A* for a responsive cell and in *B* for a nonresponsive cell. In 17 cells, however, such as the example shown in *C*, the response to kainate clearly was enhanced after Con A treatment. The experiment reported in *D* illustrates the effect of Con A treatment on the action of kainate recorded under voltage-clamp conditions (holding potential −80 mV). In five cells examined, Con A produced no enhancement of kainate-induced current or $[Ca^{2+}]_i$ increase.

kainate-activated increase in $[Ca^{2+}]_i$ also occurred when all external Na^+ was replaced with the nonpermeant cation NMDG (Holzwarth et al., 1994), although the kainate-induced inward current was greatly reduced (>90%). This suggests that the $[Ca^{2+}]_i$ signals were not attributable to Ca^{2+} influx through voltage-gated Ca^{2+} channels activated by Na^+ influx.

We also determined that the $[Ca^{2+}]_i$ signals observed were caused by Ca^{2+} influx rather than by Ca^{2+} mobilization from intracellular stores. Thus, no $[Ca^{2+}]_i$ signal was observed in Ca^{2+}-free medium (data not shown). Second, the effects of kainate were not reduced by treating cells with thapsigargin, which depletes both inositol trisphosphate-sensitive and caffeine-sensitive intracellular Ca^{2+} stores (Holzwarth et al., 1994).

Certain positively charged spider venoms such as JSTx or Argiotoxin 636 potently block only those AMPA receptors that lack GluR2(R) (Blaschke et al., 1993; Herlitze et al., 1993). Because high Ca^{2+} permeability of AMPA receptors has been associated with lack of GluR2(R), we would expect AMPA receptors that flux Ca^{2+} efficiently to be blocked by these toxins. In keeping with this expectation, we found that JSTx blocked the kainate-induced Na^+ current and $[Ca^{2+}]_i$ signal in O-2A progenitor cells (Fig. 2*A*). The kainate-activated current was 130 ± 34 pA in the absence and 39 ± 9 pA in the presence of JSTx, whereas the peak $[Ca^{2+}]_i$ increases were 504 ± 41 and 193 ± 28 nM, respectively (n = 6; all values are mean ± SEM). We were surprised to find, however, that the toxin did not block kainate-induced Na^+ currents or $[Ca^{2+}]_i$ signals very effectively after differentiation of cells into type II astrocytes (Fig. 2*B*). In these cells, the inward current induced by kainate was 416 ± 43 pA in the absence and 373 ± 43 pA in the presence of JSTx. The $[Ca^{2+}]_i$ increases were 322 ± 46 and 295 ± 42 nM, respectively (n = 6). Similar results were obtained in imaging studies carried out under Na^+-free conditions (Fig. 3). $[Ca^{2+}]_i$ increases induced by kainate in O-2A progenitors in the absence and presence of 500 nM JSTx were 716 ± 162 and 233 ± 35 nM ($p < 0.05$; n = 22), respectively, whereas in type II astrocytes they were 979 ± 206 and 873 ± 244 nM (n = 18). After the addition of serum, the sensitivity to JSTx changed slowly over a period of days. Some change already had occurred after 36 hr, and a virtually complete switch to JSTx insensitivity had occurred in a majority of cells after 1 week (Fig. 3). The $[Ca^{2+}]_i$ signal and Na^+ current were approximately equally sensitive to this toxin. It should be noted that we used very high toxin concentrations. Indeed, at the concentrations used, AMPA receptors lacking GluR2(R) examined in artificial-expression systems are blocked nearly completely (Blaschke et al., 1993; Herlitze et al., 1993), particularly at the membrane potentials prevailing in the voltage-clamp studies.

As another test of the toxin sensitivity of type II astrocyte

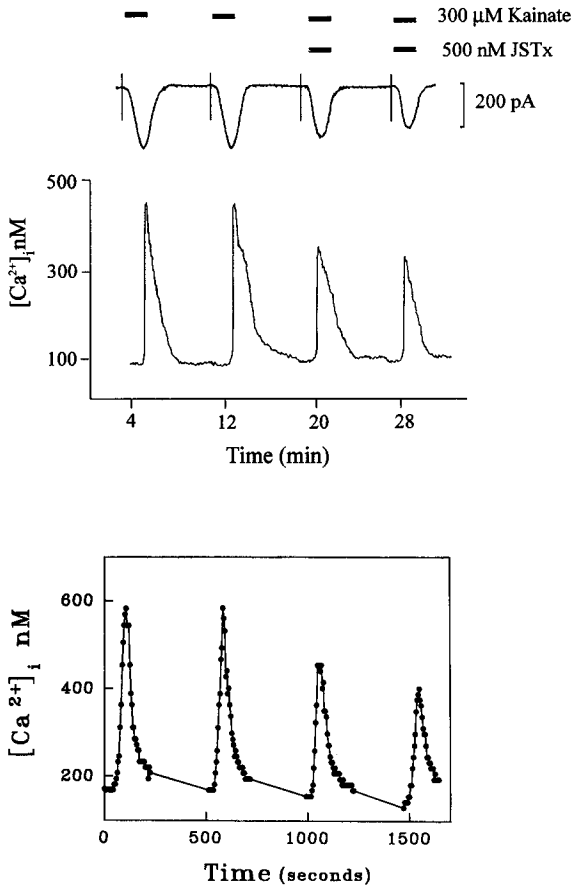

Figure 7. Effect of JSTx (500 nM) on kainate-activated responses in differentiated cortical oligodendrocytes. Representative traces of simultaneous current and $[Ca^{2+}]_i$ changes induced by kainate under voltage-clamp conditions (*top*) and of imaging experiments in Na^+-free buffer (*bottom*). Cells used in these imaging studies were identified by immunocytochemistry using gridded coverslips.

AMPA receptors, we evaluated the effect of Argiotoxin 636 on the kainate-induced Na^+ currents and Ca^{2+} signals. As with JSTx, only a modest blocking effect of Argiotoxin 636 was noted in both the voltage-clamp and the imaging studies. In these experiments, the peak kainate-activated current was 440 ± 123 pA in the absence and 316 ± 101 pA in the presence of Argiotoxin 636 (n = 6; Fig. 4). The kainate-activated $[Ca^{2+}]_i$ increase was 478 ± 63 nM in the absence and 318 ± 46 nM in the presence of Argiotoxin 636 (n = 6; Fig. 4). Similarly, imaging studies showed a 10 ± 8% (n = 4) inhibition of the kainate-activated $[Ca^{2+}]_i$ increase by Argiotoxin 636 (1 μM; data not shown). In contrast to the lack of effect of the spider toxins, we did observe that Evans blue, a compound that has been shown to block AMPA receptors that possess GluR1 and -2 (Keller et al., 1993), effectively blocked both the $[Ca^{2+}]_i$ signal and the Na^+ current to a similar extent in the type II astrocytes (Fig. 4) (kainate-activated current: 340 ± 71 pA in the absence and 70 ± 31 pA in the presence of Evans blue, n = 7; $[Ca^{2+}]_i$ increase: 352 ± 97 nM in the absence and 150 ± 44 nM in the presence of Evans blue, n = 7).

Because kainate can activate AMPA and kainate receptors (Partin et al., 1993; Patneau et al., 1994), and because both of these can potentially flux Ca^{2+} (Dingledine et al., 1992; Egebjerg and Heinemann, 1993; Kohler et al., 1993) and occur in cells of O-2A lineage (Gallo et al., 1994; Patneau et al., 1994), we determined which class of receptors was responsible for the $[Ca^{2+}]_i$ signals observed in these experiments. Under normal conditions, activation of AMPA receptors by kainate produces relatively little inactivation, whereas activation of kainate receptors by the same agonist produces currents that are extremely brief (Partin et al., 1993). Cyclothiazide can remove any inactivation of the AMPA receptors, whereas concanavalin A (Con A) has a similar potentiating effect that is relatively selective for kainate receptors (Partin et al., 1993). We observed that cyclothiazide invariably produced a large enhancement of the effects of either AMPA or kainate (Fig. 5) in type II astrocytes. In these cells, AMPA produced a peak increase in $[Ca^{2+}]_i$ of 37 ± 6 nM (n = 39) in the absence and 779 ± 67 nM (n = 8) in the presence of 10 μM cyclothiazide. Kainate produced a peak increase in $[Ca^{2+}]_i$ of 375 ± 32 nM (n = 160) in the absence and 856 ± 34 nM (n = 9) in the presence of 10 μM cyclothiazide. In contrast, incubation with Con A for lengths of time sufficient to remove kainate-receptor desensitization (Wong and Mayer, 1993) generally had very little effect (Fig. 6). In 304 cells examined by imaging the $[Ca^{2+}]_i$, response to kainate was 476 ± 25 nM in the absence and 386 ± 22 nM in the presence of Con A. Interestingly, in a few cells studied (5.6%), we did observe potentiated responses to kainate after Con A treatment (Fig. 6*C*). This is consistent with the presence of kainate receptors in a population of these cells (see also Patneau et al., 1994). This population seems to be relatively small, however, under our experimental conditions. For example, in none of the cells tested under voltage-clamp conditions (Fig. 6*D*) did we see any effect of Con A [kainate-induced current was 436 ± 118 pA in the absence and 312 ± 64 pA in the presence of Con A (n = 5)]. Although we may have underestimated the percentage of cells expressing kainate receptors, pharmacological evidence using CG-4 cells also suggests that AMPA receptors are the main species responsible for the kainate-induced $[Ca^{2+}]_i$ signal in these cells (see below).

To compare its effects in type II astrocytes, we also analyzed the effect of JSTx on kainate-induced responses in differentiated oligodendrocytes. In voltage-clamp studies, we found that JSTx partially blocked the kainate-activated current and $[Ca^{2+}]_i$ increases in these cells. As shown in Figure 7, JSTx reduced the kainate-activated current by 28 ± 7% and the $[Ca^{2+}]_i$ increase by 35 ± 9% (n = 6). The average currents induced by kainate in the absence and in the presence of JSTx were 182 ± 7 and 131 ± 6 pA, respectively. The $[Ca^{2+}]_i$ increases were 440 ± 60 and 286 ± 43 nM, respectively. The imaging experiments confirmed these results and showed that JSTx inhibited the kainate-activated $[Ca^{2+}]_i$ increase by 33 ± 5% (n = 44). The peak $[Ca^{2+}]_i$ increases were 728 ± 117 and 488 ± 42 nM in the absence and in the presence of the toxin, respectively. Thus, the inhibitory effects of JSTx in these cells were intermediate between those observed in O-2A progenitors and in type II astrocytes.

AMPA receptors and Ca^{2+} fluxes in CG-4 cells

The CG-4 cell line derives from O-2A progenitors and retains many of the features of these cells, including the presence of Ca^{2+}-permeable AMPA receptors (Louis et al., 1992; Pende et al., 1994; Holtzclaw et al., 1995). CG-4 cells also can be differentiated into cells that possess many of the morphological and antigenic features of type II astrocytes or oligodendrocytes (Louis et al., 1992; Gallo et al., 1994). When CG-4 cells were examined in voltage-clamp recordings, they behaved similarly to the primary glia cultures discussed above. Thus, both the Na^+ current and the $[Ca^{2+}]_i$ signal were blocked by JSTx in progenitor cells ($A2B5^+$,

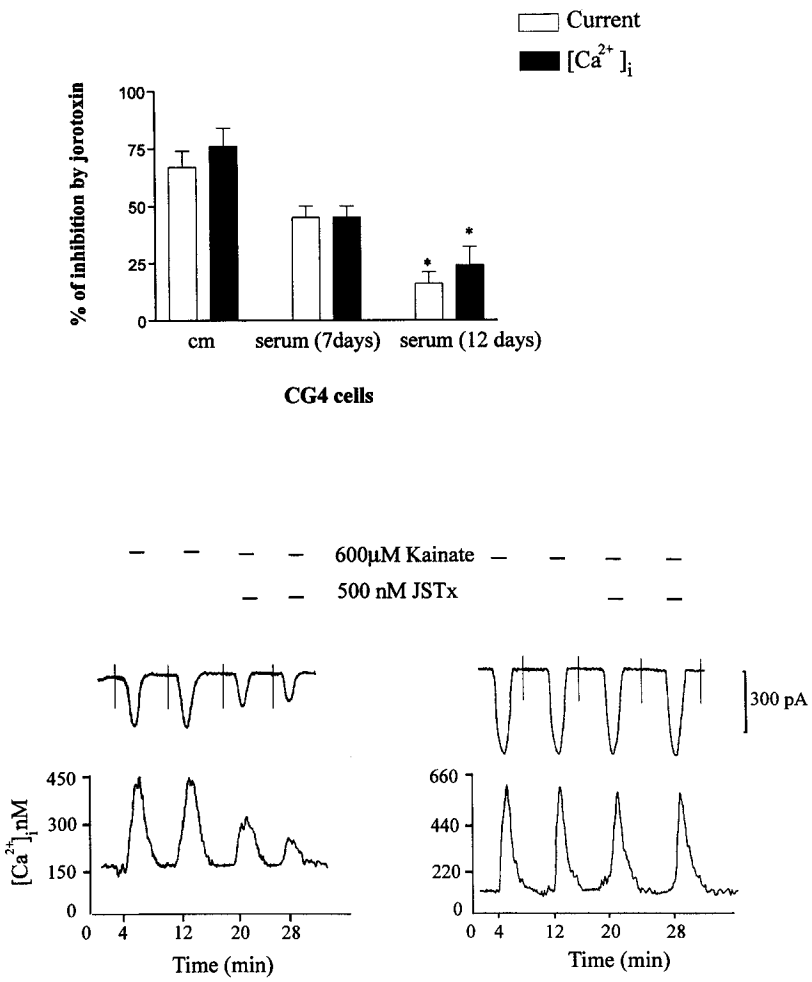

Figure 8. Simultaneous recording of the effect of JSTx on kainate-induced currents and $[Ca^{2+}]_i$ increases in CG-4 cells cultured either in a serum-free, B-104-conditioned medium (*cm*) as O-2A progenitors or in the presence of *serum* (see Materials and Methods) to allow their differentiation into type II astrocytes. *Top*, The values reported here are mean ± SEM (*$p < 0.05$ vs CG-4 cultured in serum-free medium). *Bottom*, Traces are typical examples of the responses obtained in undifferentiated (*left*) and differentiated CG-4 cells (*right*).

$GFAP^-$) (Fig. 8). The kainate-induced inward current in O-2A progenitor CG-4 cells was 120 ± 27 pA ($n = 11$) in the absence of JSTx and 35 ± 11 ($n = 7$) in the presence of JSTx. The kainate-induced $[Ca^{2+}]_i$ increase was 639 ± 55 nM in the absence of JSTx and 200 ± 39 nM in the presence of the toxin (see also Table 1 for dose–response data). Similar sensitivity to the toxin was observed in imaging studies (Fig. 9). The kainate-induced $[Ca^{2+}]_i$ increase in the absence of JSTx was 897 ± 162 nM, whereas it was 119 ± 14 nM in the presence of 500 nM JSTx ($n = 15$). Kainate-induced $[Ca^{2+}]_i$ increases were uniformly JSTx-sensitive in these cells, although the dose–response relationship for toxin sensitivity differed from cell to cell (Fig. 9; Table 2). CG-4 cells also were differentiated to produce type II astrocyte-like cells ($A2B5^+$, $GFAP^+$). Under these circumstances, the cells slowly changed their sensitivity to JSTx in a way similar to authentic O-2A progenitors, so that by 12 d many cells were completely resistant to JSTx. In differentiated CG-4 cells, the inward current activated by kainate was 240 ± 40 pA ($n = 9$) and 212 ± 31 pA ($n = 9$) in the absence or in the presence of 500 nM JSTx, respectively. The kainate-induced increases in $[Ca^{2+}]_i$ were 593 ± 46 nM in the absence of JSTx and 544 ± 29 nM in the presence of the toxin. This change in sensitivity took somewhat longer than with O-2A progenitor cells (Figs. 8, 9).

We also observed that kainate-induced $[Ca^{2+}]_i$ increases in both undifferentiated and differentiated cells were blocked completely by GYKI-53655 at concentrations at which it selectively blocks AMPA rather than kainate receptors (Fig. 10) (Paternain et al., 1995). This suggests further that AMPA receptor is the

Table 1. Dose response for the effect of JSTx on kainate (600 μM)-induced inward current and $[Ca^{2+}]_i$ increase, recorded simultaneously under voltage-clamp conditions (HP = −80 mV) in CG-4 progenitor cells ($n = 12$)

Jorotoxin (nM)	% Inhibition of peak current	% Inhibition of peak Ca^{2+}
1	23 ± 7	35 ± 8
10	40 ± 6	50 ± 6
100	65 ± 7	60 ± 8
500	70 ± 7	79 ± 8

Table 2. Dose response for the effect of JSTx on kainate (600 μM)-induced $[Ca^{2+}]_i$ increase in CG-4 progenitor cells, studied by Fura-2 video imaging

Jorotoxin (nM)	Responsive cells (%)	% Inhibition of peak $[Ca^{2+}]_i$
1	50 ($n = 14$)	28 ± 4
10	90 ($n = 15$)	50 ± 6
100	100 ($n = 12$)	77 ± 3
500	100 ($n = 15$)	87 ± 8

The responsive cells column represents the percentage of cells significantly inhibited by JSTx for each concentration used.

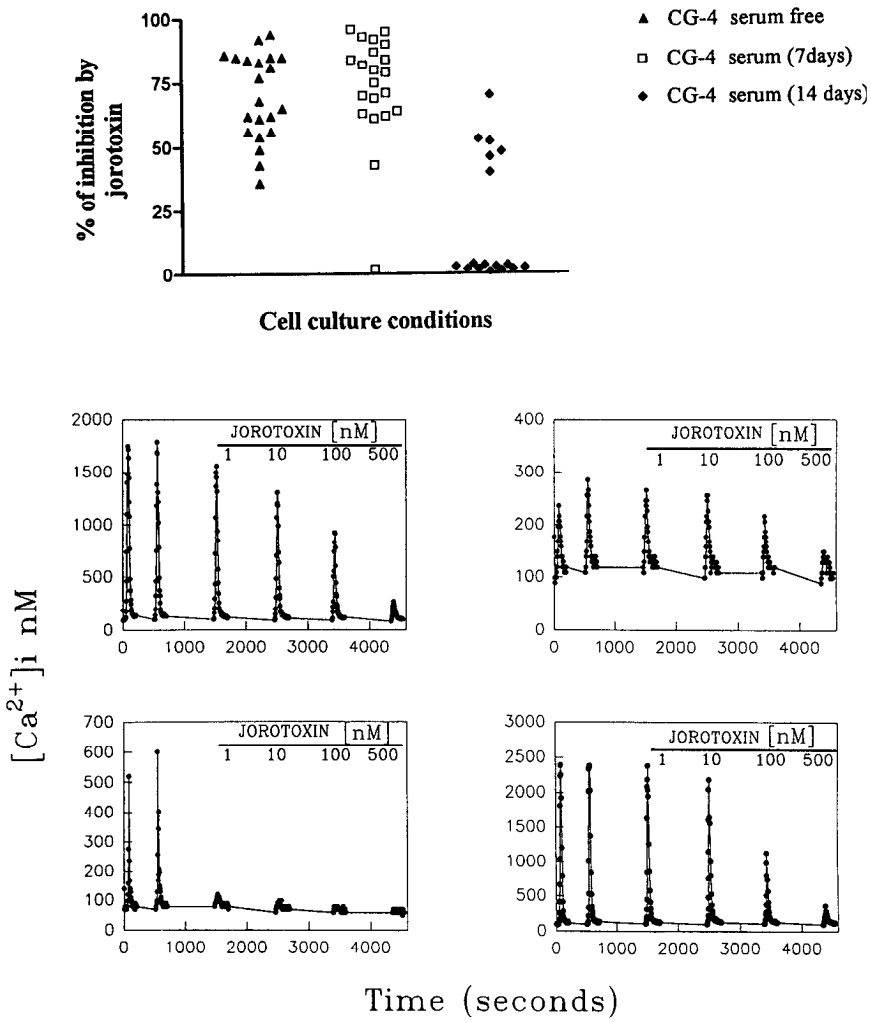

Figure 9. *Top*, Effect of JSTx on the peak kainate (600 μM)-induced $[Ca^{2+}]_i$ increase in CG-4 cells during differentiation. Although the magnitude of the inhibitory effect of JSTx (500 nM) was quite variable from cell to cell (ranging from 30 to >90%), it was always observed in the O-2A progenitor CG-4 cells (serum-free culture conditions; ▲) and in most of the cells after 1 week in serum (■), whereas the toxin was almost completely ineffective on a majority of CG-4 differentiated into type II astrocytes (inhibition, 19 ± 6% after 14 d in serum; ◆). Each data point is from a single cell. *Bottom*, Dose responses for the effect of JSTx on the $[Ca^{2+}]_i$ increase caused by kainate in O-2A progenitor CG-4 cells (see also Table 1). The four different traces are from single cells and are representative of the different sensitivities of cells to JSTx.

major subtype responsible for the kainate-activated $[Ca^{2+}]_i$ signals.

As with primary cultures, we observed intermediate blocking effects of JSTx in CG-4-derived oligodendrocyte-like cells (Fig. 11). The kainate-induced currents and $[Ca^{2+}]_i$ increases were reduced by 32 ± 4 and 49 ± 7% by JSTx, respectively, in voltage-clamp experiments (n = 7). The kainate-activated current was 128 ± 8 pA in the absence of JSTx and 87 ± 7 pA in the presence of the toxin. The increase in $[Ca^{2+}]_i$ induced by kainate alone was 550 ± 45 nM, and it was 280 ± 21 nM in the presence of JSTx. Imaging studies showed that JSTx produced a 58 ± 6% inhibition of the kainate-induced $[Ca^{2+}]_i$ increase. In these experiments, the $[Ca^{2+}]_i$ increase induced by kainate was 975 ± 104 nM in the absence of JSTx and 410 ± 40 nM in its presence (n = 45).

The diverse blocking effects of JSTx in progenitors, type II astrocytes, and oligodendrocytes suggested some alteration in the subunit composition of AMPA receptors in these cell types. We investigated this possibility using Western blot analysis. As was reported previously by others (Gallo et al., 1994; Patneau et al., 1994; Puchalski et al., 1994), we observed the presence of GluR2, GluR3, and GluR4 in CG-4 cells (Fig. 12). The relative levels of expression of each of these subunits changed on differentiation. Densitometric analysis of the immunoblots showed a large increase in the level of GluR2 when cells were differentiated into type II astrocyte-like cells (ratio of type II to O-2A progenitors was 2.62) and a slight increase when they were differentiated into oligodendrocytes (ratio of oligodendrocytes to O-2A progenitors was 1.27). The levels of GluR3 were increased slightly in type II-like cells and in oligodendrocytes (ratio of type II to O-2A was 1.50; ratio of oligodendrocytes to O-2A was 1.45). The levels of GluR4 also were higher in type II astrocytes and oligodendrocytes (ratio of type II to O-2A was 2.14; ratio of oligodendrocytes to O-2A was 5.54). The increase in GluR4 expression presumably is caused by increases in GluR4 mRNA observed under these conditions, as reported previously by Patneau et al. (1994).

DISCUSSION

The results obtained in these studies are of interest for three distinct reasons. First, we noted a change in toxin sensitivity of the AMPA receptors in O-2A progenitor cells as they differentiated into oligodendrocytes and type II astrocytes. Second, it is striking that although the AMPA receptors in type II astrocytes are resistant to the effects of JSTx, they still flux Ca^{2+} efficiently. Third, we also find that these changes in toxin sensitivity are accompanied by an increase in the levels of GluR2.

AMPA receptors in several types of neurons (Murphy and Miller, 1989a,b; Gilbertson et al., 1991; Brorson et al., 1992; Jonas et al., 1994; Lerma et al., 1994) and glia (Müller et al., 1992; Holzwarth et al., 1994; Jabs et al., 1994; Holtzclaw et al., 1995) are appreciably permeable to Ca^{2+}. The precise subunit composition of these receptors, however, has not been elucidated in most instances. Results obtained from the expression of cloned recep-

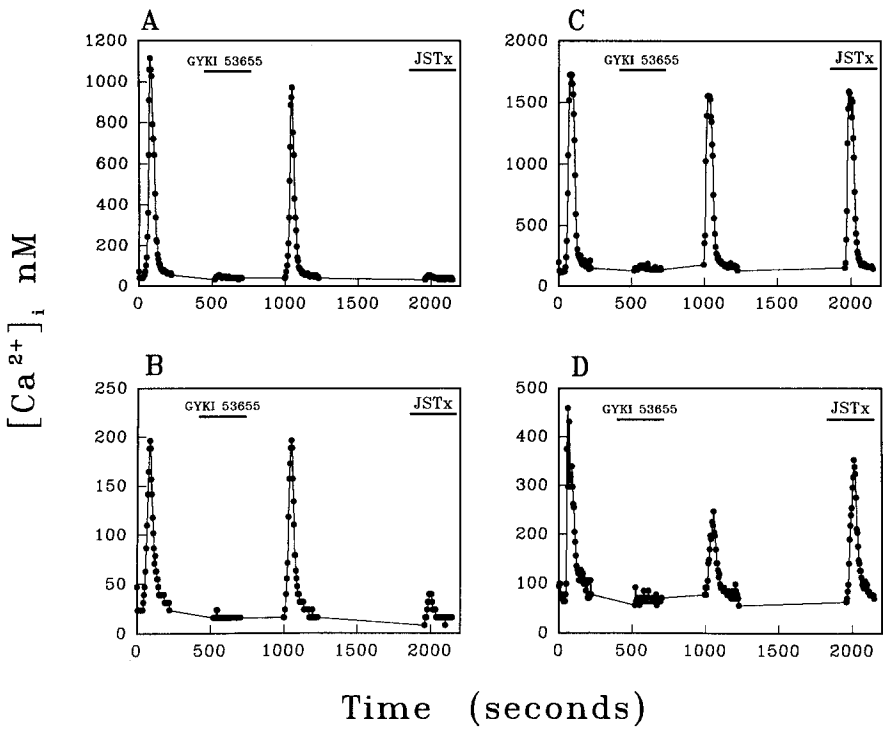

Figure 10. Effect of GYKI-53655, a selective inhibitor of AMPA receptors, on the increase in $[Ca^{2+}]_i$ evoked by kainate (600 μM) in CG-4 progenitor cells (*A*, *B*) and in type II astrocyte CG-4 cells (*C*, *D*). It can be seen clearly that, typical of all undifferentiated and differentiated cells analyzed (n = 4 and 5, respectively), 10 μM GYKI-53655 completely and reversibly blocked the kainate response, whereas only CG-4 progenitor cells were sensitive to the inhibitory action of JSTx (500 nM).

tors in artificial expression systems have demonstrated that the presence of GluR2(R) is a major determinant of the Ca^{2+} permeability of AMPA receptors (Hollmann et al., 1991; Sommer et al., 1991; Burnashev et al., 1992b, 1995). Thus, recombinant receptors expressed *in vitro* without this subunit show high Ca^{2+} permeability and current–voltage curves that are inwardly rectifying. The AMPA receptors in some cells (type II hippocampal pyramidal neurons and Bergmann glial cells) show precisely these properties (Iino et al., 1990; Ozawa et al., 1991; Burnashev et al., 1992b; Müller et al., 1992). In other situations, however, cells appear to possess AMPA receptors that show high Ca^{2+} permeability but straight or outwardly rectifying current–voltage curves (Schneggenburger et al., 1993a,b; Holzwarth et al., 1994; Lerma et al., 1994; Geiger et al., 1995). Estimates for the relative Ca^{2+} permeability of AMPA receptors in different cell types range from values that approach those for NMDA receptors [e.g., Bergmann glia and type II hippocampal neurons (Iino et al., 1990; Müller et al., 1992), and dentate gyrus basket cells, hilar interneurons, and auditory relay neurons (Geiger et al., 1995)] to values that are extremely low [e.g., cerebellar granule cells (Wyllie and Cull-Candy, 1994) and CA3 pyramidal cells (Geiger et al., 1995) (see below)].

How can these various observations be reconciled with each other and with data from the present experiments? It is reasonable to suppose that in cases in which GluR2(R) subunits are totally absent, the resulting AMPA receptors will show high Ca^{2+} permeability and inward rectification, as predicted from expression studies in artificial systems (Burnashev et al., 1992b; Geiger et al., 1995). This is certainly the case for type II hippocampal pyramidal neurons (Bochet et al., 1994) and Bergmann glia (Burnashev et al., 1992a; Geiger et al., 1995). Jonas et al. (1994) demonstrated that in rat neocortical nonpyramidal neurons, AMPA receptors showed a relatively high Ca^{2+} permeability. Single-cell PCR studies indicated that these cells did contain some GluR2(R), although apparently at lower levels than in neocortical pyramidal neurons, which possessed AMPA receptors with very low Ca^{2+} permeability, investigated under similar conditions. These studies were extended recently by Geiger et al. (1995), who demonstrated the correlation between GluR2 content and Ca^{2+} permeability in a range of central neurons. In our previous studies on O-2A progenitor cells (Holzwarth et al., 1994), we showed that the AMPA receptors present clearly were permeable to Ca^{2+} (and Co^{2+}) and showed little inward rectification. We suggested that a majority of the Ca^{2+} flux observed was attributable to a small number of the AMPA receptors present that did not possess GluR2(R), whereas a majority of those present did possess GluR2(R). The results of the present set of studies, however, show clearly that this original hypothesis must be wrong. If two such populations of receptors were present, then JSTx or Argiotoxin 636 would have blocked the kainate-induced $[Ca^{2+}]_i$ signal much more effectively than the Na^+ current measured simultaneously; however, this was not found to be the case. Even when used at high concentrations, the toxins had very little inhibitory effect on either Na^+ currents or Ca^{2+} fluxes in type II astrocytes and reduced both parameters to a similar extent in oligodendrocytes and progenitors. The lack of effect of the spider toxins on type II astrocytes suggests that the receptors responsible for both the Na^+ and the Ca^{2+} fluxes in these cells are actually the same or, at the very least, that they all contain GluR2(R). This conclusion is supported also by the blocking effects of Evans blue. Although this latter compound in no way can be considered specific, our results are consistent with those of Keller et al. (1994), who demonstrated that Evans blue blocked AMPA receptors that contained GluR2(R). Interestingly, the Na^+ currents and Ca^{2+} fluxes in the O-2A progenitor cells and progenitor CG-4 cells displayed high sensitivity to spider toxins, whereas oligodendrocytes displayed an intermediate sensitivity. We also found that the relative amounts of GluR2 in these cells correlated with increasing resistance to block by JSTx.

The reason that AMPA receptors are both Ca^{2+}-impermeable

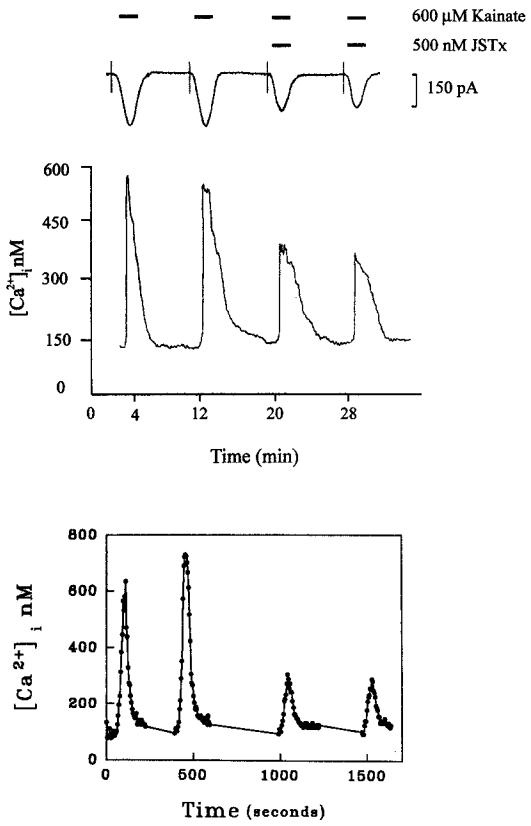

Figure 11. Simultaneous recording of the effect of JSTx (500 nM) on the kainate-induced current and $[Ca^{2+}]_i$ increase in CG-4 cells differentiated into oligodendrocytes showed a partial inhibitory effect of the toxin on both parameters (*top*). Similar results were obtained by $[Ca^{2+}]_i$-imaging studies (*bottom*).

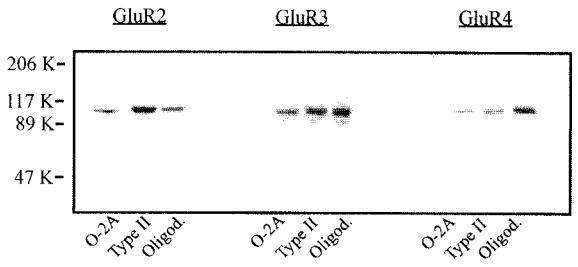

Figure 12. Western blot analysis of the expression of GluR2, GluR3, and GluR4 AMPA-receptor subunits in O-2A progenitor CG-4 (*O-2A*), type II astrocyte CG-4 (*Type II*), and oligodendrocyte CG-4 cells (*Oligod.*). Proteins (30 μg/lane) were run on 7.5% SDS-PAGE minigels, and membranes were incubated for 1 hr with monoclonal antibody for GluR2 or polyclonal antibodies for GluR3 and GluR4. Figure shows one of two similar experiments.

and resistant to block by positively charged toxins such as JSTx and Argiotoxin 636 may be that these receptors are repelled by the additional positive charge provided by the Arg residue found in the edited subunit, GluR2(R). Similar considerations apply to the actions of other positively charged species such as polyamines (Koh et al., 1995). This Arg residue probably is located in close proximity to the ion permeability pore (Burnashev et al., 1992b; Hollmann and Heinemann, 1994). If each AMPA receptor consists of approximately five subunits (by analogy with nicotinic receptors; Wenthold et al., 1992), then as many as five of these positive charges could be found in the limiting condition if homomeric GluR2(R) channels were formed. This situation is unlikely to occur in practice, however, because GluR2(R) subunits presumably are found in combination with other AMPA-receptor subunits (Petralia and Wenthold, 1992; Gallo et al., 1994; Jonas et al., 1994; Patneau et al., 1994; Puchalski et al., 1994; Geiger et al., 1995). It is likely, therefore, that the Ca^{2+} permeability and toxin sensitivity of AMPA receptors are caused not only by the absolute presence or absence of GluR2(R) but also by exactly how many of these subunits and, thus, how many extra positive charges are present in the receptor complex. Expression studies in artificial systems using GluR2(R) mixed with other AMPA-receptor subunits have demonstrated clearly that the degree of Ca^{2+} permeability and sensitivity to block by spider toxins can be changed differentially by altering not only the types of subunits used but also their relative proportions (Burnashev et al., 1992b, 1995; Blaschke et al., 1993; Herlitze et al., 1993). A similar result is implied by the data of Jonas et al. (1994) and Geiger et al. (1995). In their recent studies on the composition and properties of AMPA receptors in a range of central nervous system neurons, Geiger et al. (1995) found a marked correlation between the abundance of GluR2 in cells and decreasing Ca^{2+} permeability. These authors suggested that the presence of even a single GluR2 subunit in the receptor complex was enough to decrease Ca^{2+} permeability significantly. It may be that a single GluR2 also greatly reduces the sensitivity of the receptor to block by JSTx.

The present results suggest that, at least in type II astrocytes, no mosaic of receptors occurs that includes highly Ca^{2+}-permeable GluR2(R)-negative complexes. The receptors present all appear to contain GluR2(R) but also to exhibit an appreciable Ca^{2+} permeability. We cannot rule out the possibility, however, that mosaics of highly Ca^{2+}-permeable and -impermeable AMPA receptors occur in other cell types. For example, this situation may exist in the undifferentiated progenitors and in oligodendrocytes. The relative amounts of the different types of receptors would be controlled by the relative levels of GluR2 that increase on differentiation, as shown in this study. Our results are consistent with those in the literature reporting an entire range of relative Ca^{2+} permeabilities (P) for AMPA receptors in different cell types ($P_{Ca^{2+}}/P_{X^+}$ ranging from 0.01 to 2.7) (Mayer and Westbrook, 1987; Iino et al., 1990; Ozawa et al., 1991; Burnashev et al., 1992a,b; Jonas and Sakmann, 1992; Schneggenburger et al., 1993a,b; Jonas et al., 1994; Wyllie and Cull-Candy, 1994; Geiger et al., 1995). These results could be attributable to the presence of AMPA receptors containing different relative amounts of GluR2(R) and, consequently, different Ca^{2+} permeabilities. Thus, the Ca^{2+} permeabilities of AMPA receptors in normal cells actually may form a continuum of values allowing for very fine tuning of glutamate-activated Ca^{2+} fluxes.

In conclusion, the reason that the toxin sensitivity of AMPA receptors decreases when O-2A cells differentiate into oligodendrocytes and, particularly, into type II astrocytes may be attributable to a change in the AMPA-receptor subunit composition so that a higher proportion of receptors contains GluR2(R). This conclusion is consistent with the biochemical results reported in this study. The relevance of these studies for events occurring *in vivo* is indicated by a recent report demonstrating the "intermediate" Ca^{2+} permeability of "complex" glial cells in mouse hippocampal slices (Seifert and Steinhauser, 1995).

REFERENCES

Blaschke M, Keller B, Rivosecchi R, Hollmann M, Heinemann S, Konnerth A (1993) A single amino acid determines the subunit specific spider toxin block of α-amino-3-hydroxy-5-methyl-4-propionate/kainate receptor channels. Proc Natl Acad Sci USA 90:6528–6532.

Bliss TVP, Collingridge GL (1993) A synaptic model of memory: long-term potentiation in the hippocampus. Nature 361:31–39.

Bochet P, Audinet E, Lambolez B, Crepel F, Rossier J, Iino M, Tsuzuki K, Ozawa S (1994) Subunit composition at the single cell level explains functional properties of a glutamate gated channel. Neuron 12:383–388.

Brorson JR, Bleakman D, Chard PS, Miller RJ (1992) Calcium directly permeates the kainate/AMPA receptors in cultured cerebellar Purkinje neurons. Mol Pharmacol 41:603–608.

Burnashev N, Khodorova A, Jonas P, Helm PJ, Wisden W, Monyer H, Seeburg PH, Sakmann B (1992a) Calcium permeable AMPA receptors in fusiform cerebellar glial cells. Science 256:1566–1570.

Burnashev N, Monyer H, Seeburg P, Sakmann B (1992b) Divalent ion permeability of AMPA receptor channels is dominated by the edited form of a single subunit. Neuron 8:189–198.

Burnashev N, Zhou Z, Neher E, Sakmann B (1995) Fractional calcium current through recombinant GluR channels of the NMDA, AMPA and kainate receptor subtypes. J Physiol (Lond) 485:403–418.

Choi DW, Rothman SM (1990) The role of glutamate neurotoxicity in hypoxic-ischemic neuronal death. Annu Rev Neurosci 13:171–182.

Dingledine R, Hume RI, Heinemann SF (1992) Structural determinants of barium permeation and rectification in non-NMDA glutamate receptor channels. J Neurosci 12:4080–4087.

Egebjerg J, Heinemann SF (1993) Ca permeability of edited and unedited versions of the kainate selective glutamate receptor GluR6. Proc Natl Acad Sci USA 90:755–759.

Gallo V, Patneau DK, Mayer ML, Vaccarino FM (1994) Excitatory amino acid receptors in glial progenitor cells' molecular and functional properties. Glia 11:94–101.

Geiger JRP, Melcher T, Koh D-S, Sakmann B, Seeburg PH, Jonas P, Monyer H (1995) Relative abundance of subunit mRNAs determines gating and Ca^{2+} permeability of AMPA receptors in principal neurons and interneurons in rat CNS. Neuron 15:193–204.

Gilbertson TA, Scobey R, Wilson M (1991) Permeation of calcium ions through non-NMDA glutamate channels in retinal bipolar cells. Science 251:1613–1615.

Grynkiewicz G, Poenie M, Tsien RY (1985) A new generation of Ca^{2+} indicators with greatly improved fluorescence properties. J Biol Chem 260:3440–3450.

Herlitze S, Raditsch M, Ruppersberg JP, Jahn W, Monyer H, Schoepfer R, Witzemann V (1993) Argiotoxin detects molecular differences in AMPA receptor channels. Neuron 10:1131–1140.

Hollmann M, Hartley M, Heinemann S (1991) Ca permeability of KA-AMPA gated glutamate receptor channels depends on subunit composition. Science 252:851–853.

Hollmann M, Heinemann S (1994) Cloned glutamate receptors. Annu Rev Neurosci 17:31–108.

Holtzclaw LA, Gallo V, Russell JT (1995) AMPA receptors shape Ca^{2+} responses in cortical oligodendrocyte progenitors and CG-4 cells. J Neurosci Res 42:124–130.

Holzwarth JA, Gibbons SJ, Brorson JR, Philipson LH, Miller RJ (1994) Glutamate receptor agonists stimulate diverse calcium responses in different types of cultured rat cortical glial cells. J Neurosci 14:1879–1891.

Hume RI, Dingledine R, Heinemann S (1991) Identification of a site in glutamate receptor subunits that controls calcium permeability. Science [Suppl] 253:1028–1031.

Iino M, Ozawa S, Tsuzuki K (1990) Permeation of calcium through excitatory amino acid receptor channels in cultured rat hippocampal neurones. J Physiol (Lond) 424:151–165.

Jabs R, Kirchhoff F, Kettenmann H, Steinhauser C (1994) Kainate activates Ca permeable glutamate receptors and blocks voltage gated K currents in glial cells of mouse hippocampal slices. Pflügers Arch 426:310–319.

Jonas P, Racca C, Sakmann B, Seeburg PH, Monyer H (1994) Differences in Ca permeability of AMPA type glutamate receptor channels in neocortical neurons caused by differential GluR B subunit expression. Neuron 12:1281–1289.

Jonas P, Sakmann B (1992) Glutamate receptor channels in isolated patches from CA1 and CA3 pyramidal cells of rat hippocampal slices. J Physiol (Lond) 455:143–171.

Keller BU, Blascke M, Rivosecchi R, Hollmann M, Heinemann SF, Konnerth A (1993) Identification of a subunit specific antagonist of α-amino-3-hydroxy-5-methyl-4-isoxazolepropionate/kainate receptor channels. Proc Natl Acad Sci USA 90:605–609.

Koh D-J, Burnashev N, Jonas P (1995) Block of native Ca^{2+} permeable AMPA receptors in rat brain by intracellular polyamines generates double rectification. J Physiol (Lond) 486:305–312.

Kohler M, Burnashev N, Sakmann B, Seeburg PH (1993) Determinants of Ca permeability in both TM1 and TM2 of high affinity kainate receptor channels diversity by RNA editing. Neuron 10:491–500.

Laemmli UK (1970) Cleavage of structural proteins during the assembly of the head of bacteriophage T4. Nature 227:680–685.

Lambolez B, Audinat E, Bochet P, Crepel F, Rossier J (1992) AMPA receptor subunits expressed by single Purkinje cells. Neuron 9:247–258.

Lerma J, Morales M, Ibarz JM, Somohano F (1994) Rectification properties and Ca^{2+} permeability of glutamate receptor channels in hippocampal cells. Eur J Neurosci 6:1080–1088.

Louis JC, Magal E, Muir D, Manthorpe M, Varon S (1992) CG-4, a new bipotential cell line from rat brain, is capable of differentiating *in vitro* into either mature oligodendrocytes or type-2 astrocytes. J Neurosci Res 31:193–204.

MacDermott AB, Mayer ML, Westbrook GL, Smith SJ, Barker JL (1986) NMDA-Receptor activation increases cytoplasmic calcium concentration in cultured spinal cord neurons voltage clamp. Nature 321:519–522.

Mayer ML, Westbrook GL (1987) Permeation and block of *N*-methyl-D-aspartic acid receptor channels by divalent cations in cultured mouse central neurons. J Physiol (Lond) 394:501–527.

Mayer ML, MacDermott AB, Westbrook GL, Smith SJ, Barker JL (1987) Agonist- and voltage-gated calcium entry in cultured mouse spinal cord neurons under voltage clamp measured using Arsenazo III. J Neurosci 7:3230–3244.

McBain CJ, Mayer ML (1994) *N*-Methyl-D-aspartic acid receptor structure and function. Physiol Rev 74:723–760.

McCarthy KD, de Vellis J (1980) Preparation of separate astroglial and oligodendroglia cell cultures from rat cerebral tissue. J Cell Biol 85:890–902.

Miller RJ (1994) G-protein linked glutamate receptors. Semin Neurosci 6:105–115.

Müller T, Moller T, Berger T, Schnitzer J, Kettenmann H (1992) Calcium entry through kainate receptors and resulting potassium channel blockade in Bergmann glial cells. Science 256:1563–1566.

Murphy SN, Miller RJ (1989a) Regulation of Ca influx into striatal neurons by kainic acid. J Pharmacol Exp Ther 249:184–193.

Murphy SN, Miller RJ (1989b) Two distinct quisqualate receptors regulate Ca homeostasis in hippocampal neurons *in vitro*. Mol Pharmacol 35:671–680.

Ozawa S, Iino M, Tsuzuki K (1991) Two types of kainate response in cultured rat hippocampal neurons. J Neurophysiol 66:2–11.

Partin KM, Patneau DK, Winters CA, Mayer ML, Buonanno A (1993) Selective modulation of desensitization at AMPA versus kainate receptors by cyclothiazide and concanavalin A. Neuron 11:1069–1082.

Paternain AV, Morales M, Lerma J (1995) Selective antagonism of AMPA receptors unmasks kainate receptor mediated responses in hippocampal neurons. Neuron 14:185–189.

Patneau DK, Wright PW, Winters C, Mayer ML, Gallo V (1994) Glial cells of the oligodendrocyte lineage express both kainate and AMPA preferring subtypes of glutamate receptor. Neuron 12:357–371.

Pende M, Holtzclaw LA, Curtis JL, Russell JT, Gallo V (1994) Glutamate regulates intracellular calcium and gene expression in oligodendrocyte progenitors through the activation of DL-α-amino-3-hydroxy-5-methyl-4-isoxazolepropionic acid receptors. Proc Natl Acad Sci USA 91:3215–3219.

Petralia RS, Wenthold RJ (1992) Light and electron immunocytochemical localization of AMPA selective glutamate receptors in the rat brain. J Comp Neurol 318:329–334.

Pichalski RB, Louis JC, Brose N, Traynelis SF, Egebjerg J, Kukekov V, Wenthold RJ, Rogers SW, Lin F, Moran T, Morrison JH, Heinemann SF (1994) Selective RNA editing and subunit assembly of native glutamate receptors. Neuron 13:131–146.

Schneggenburger R, Tempia F, Konnerth A (1993a) Glutamate and AMPA mediated calcium influx through glutamate receptor channels in medial septal neurons. Neuropharmacology 32:1221–1228.

Schneggenburger R, Zhou Z, Konnerth A, Neher E (1993b) Fractional contribution of calcium to the cation current through glutamate receptor channels. Neuron 11:133–143.

Seifert G, Steinhauser C (1995) Glial cells in the mouse hippocampus express AMPA receptors with an intermediate Ca^{2+} permeability. Eur J Neurosci 7:1872–1881.

Sommer B, Kohler M, Sprengel R, Seeburg PH (1991) RNA editing in brain controls a determinant of ion flux in glutamate fated channels. Cell 67:11–20.

Thayer SA, Sturek M, Miller RJ (1988) Measurement of neuronal Ca transients using simultaneous microfluorimetry and electrophysiology. Pflügers Arch 412:216–223.

Towbin H, Staehelin T, Gordon J (1979) Electrophoretic transfer of protein from polyacrylamide gels to nitrocellulose sheets: procedure and some applications. Proc Natl Acad Sci USA 76:4350–4354.

Wenthold RJ, Yokotani N, Doi K, Wade K (1992) Immunochemical characterization of the non-NMDA glutamate receptor using subunit-specific antibodies. J Biol Chem 267:501–507.

Wong LA, Mayer ML (1993) Differential modulation by cyclothiazide and concanavalin A of desensitization at AMPA and kainate preferring glutamate receptors. Mol Pharmacol 44:504–510.

Wyllie DJA, Cull-Candy SG (1994) A comparison of non-NMDA receptor channels in type-2 astrocytes and granule cells from rat cerebellum. J Physiol (Lond) 475:95–114.

Zeilhofer HU, Müller T, Swandulla D (1993) Inhibition of voltage sensitive Ca channels by L-glutamate receptor mediated calcium influx. Neuron 10:879–887.